HHS Public Access

Author manuscript

Cancer Res. Author manuscript; available in PMC 2019 May 28.

Published in final edited form as:

Cancer Res. 2018 May 01; 78(9): 2383–2395. doi:10.1158/0008-5472.CAN-17-1672.

Cross-talk Signaling between HER3 and HPV16 E6 and E7 Mediates Resistance to PI3K Inhibitors in Head and Neck Cancer

Toni M. Brand[1], **Stefan Hartmann**[1,2], **Neil E. Bhola**[1], **Hua Li**[1], **Yan Zeng**[1], **Rachel A. O'Keefe**[1], **Max V. Ranall**[3], **Sourav Bandyopadhyay**[3], **Margaret Soucheray**[4], **Nevan J. Krogan**[4], **Carolyn Kemp**[5], **Umamaheswar Duvvuri**[5], **Theresa LaVallee**[6], **Daniel E. Johnson**[1], **Michelle A. Ozbun**[7], **Julie E. Bauman**[8], and **Jennifer R. Grandis**[1]

[1]Department of Otolaryngology - Head and Neck Surgery, University of California San Francisco, San Francisco, California.

[2]Department of Oral and Maxillofacial Plastic Surgery, University Hospital Würzburg, Würzburg, Germany.

[3]Department of Bioengineering and Therapeutic Sciences, University of California San Francisco, San Francisco, California.

[4]Department of Cellular and Molecular Pharmacology, University of California San Francisco, San Francisco, California.

[5]Department of Otolaryngology, University of Pittsburgh School of Medicine, Pittsburgh, Pennsylvania.

[6]Celldex Therapeutics, New Haven, Connecticut.

[7]Department of Molecular Genetics & Microbiology, University of New Mexico School of Medicine, Albuquerque, New Mexico.

[8]Division of Hematology/Oncology, University of Arizona Cancer Center, Tucson, Arizona.

Abstract

Human papillomavirus (HPV) type 16 is implicated in approximately 75% of head and neck squamous cell carcinomas (HNSCC) that arise in the oropharynx, where viral expression of the E6

Corresponding Author: Jennifer R. Grandis, University of California San Francisco, San Francisco, CA 94105. Phone: 415-514-8086; Fax: 415-514-8520; jennifer.grandis@ucsf.edu.

Authors' Contributions

Conception and design: T.M. Brand, N.E. Bhola, M.V. Ranall, N.J. Krogan, T. LaVallee, M.A. Ozbun, J.E. Bauman, J.R. Grandis

Development of methodology: T.M. Brand, M.V. Ranall, U. Duvvuri, T. LaVallee

Acquisition of data (provided animals, acquired and managed patients, provided facilities, etc.): T.M. Brand, S. Hartmann, N.E. Bhola, H. Li, Y. Zang, M.V. Ranall, M. Soucheray, C. Kemp

Analysis and interpretation of data (e.g., statistical analysis, biostatistics, computational analysis): T.M. Brand, S. Hartmann, N.E. Bhola, M.V. Ranall, U. Duvvuri, T. LaVallee, M.A. Ozbun, J.E. Bauman

Writing, review, and/or revision of the manuscript: T.M. Brand, S. Hartmann, N.E. Bhola, S. Bandyopadhyay, U. Duvvuri, T. LaVallee, D.E. Johnson, M.A. Ozbun, J.E. Bauman, J.R. Grandis

Administrative, technical, or material support (i.e., reporting or organizing data, constructing databases): T.M. Brand, R.A. O'Keefe, S. Bandyopadhyay

Study supervision: T.M. Brand, N.J. Krogan, J.R. Grandis

Disclosure of Potential Conflicts of Interest

No potential conflicts of interest were disclosed.

Supplementary data for this article are available at Cancer Research Online (http://cancerres.aacrjournals.org/).

and E7 oncoproteins promote cellular transformation, tumor growth, and maintenance. An important oncogenic signaling pathway activated by E6 and E7 is the PI3K pathway, a key driver of carcinogenesis. The PI3K pathway is also activated by mutation or amplification of PIK3CA in over half of HPV(+) HNSCC. In this study, we investigated the efficacy of PI3K-targeted therapies in HPV(+) HNSCC preclinical models and report that HPV(+) cell line- and patient-derived xenografts are resistant to PI3K inhibitors due to feedback signaling emanating from E6 and E7. Receptor tyrosine kinase profiling indicated that PI3K inhibition led to elevated expression of the HER3 receptor, which in turn increased the abundance of E6 and E7 to promote PI3K inhibitor resistance. Targeting HER3 with siRNA or the mAb CDX-3379 reduced E6 and E7 abundance and enhanced the efficacy of PI3K-targeted therapies. Together, these findings suggest that cross-talk between HER3 and HPV oncoproteins promotes resistance to PI3K inhibitors and that cotargeting HER3 and PI3K may be an effective therapeutic strategy in HPV(+) tumors.

Significance—These findings suggest a new therapeutic combination that may improve outcomes in HPV(+) head and neck cancer patients.

Introduction

Human papillomaviruses (HPV) are double-stranded DNA viruses that infect the basal layer of squamous epithelia. Over 120 types of HPV have been identified, and 15 are considered to be high-risk viruses that promote cellular growth and transformation (1, 2). HPV type 16 infection is implicated in approximately 75% of head and neck squamous cell carcinomas (HNSCC) that arise in the oropharynx (3, 4). Historically, the main risk factors for HNSCC have been alcohol and/or tobacco consumption; however, over the past three decades the incidence of carcinogen-induced HNSCC has been slowly declining while HPV(+) HNSCC have increased by 225% (3–5). This epidemiologic shift to virally induced disease is associated with a younger patient population who demonstrate a generally more favorable prognosis than patients with HPV(−) tumors (6, 7). Nevertheless, approximately 25% of HPV(+) HNSCC are lethal, underscoring the need for more effective treatments (6–9).

HPV(+) HNSCCs are molecularly distinct from HPV(−) tumors due to viral expression of the E6 and E7 oncoproteins (10–12). E6 and E7 promote carcinogenesis by binding to and inducing the degradation of tumor suppressor proteins in epithelial cells (13). Specifically, E6 and E7 cause the proteasomal degradation of p53 and the retinoblastoma protein (pRb), respectively (14, 15). The oncogenic PI3K pathway, which leads to enhanced cell survival, growth, migration, and altered metabolism (16), is activated by oncogenic HPVs at multiple stages of infection and tumorigenesis (17–20). E6 and E7 activate PI3K pathway signaling by increasing receptor tyrosine kinase (RTK) expression and stability (21–25), inhibiting regulatory phosphatases (26, 27), and degrading miRNAs that play a role in PI3K pathway suppression (28, 29). Consistent with these findings, we recently reported that E6 and E7 induce the expression of the HER family receptor HER3 in HPV(+) HNSCCs (25). HER3 binds PI3K and activates the pathway in HPV(+) cells (25). In addition, the two downstream mediators of PI3K signaling, AKT, and ribosomal protein S6 (rpS6), are phosphorylated in greater than 60% of HPV(+) HNSCCs (30). Finally, the PI3K pathway is frequently activated in HPV(+) tumors by mutation and/or amplification of *PIK3CA,* the gene that encodes the p110a catalytic subunit of PI3K (31). These cumulative findings demonstrate

that the PI3K pathway is commonly activated in HPV(+) tumors through multiple mechanisms.

As the PI3K pathway plays a central role in tumorigenesis and is activated in HPV(+) HNSCC, patients with HPV(+) tumors are currently being enrolled on clinical trials testing PI3K inhibitors. In the current study, we compared the efficacy of PI3K inhibitors in HPV(+) versus HPV(−) HNSCC preclinical models. Despite the biologic rationale for targeting PI3K in HPV(+) tumors, we found that HPV(+) HNSCC cell lines and patient-derived xenografts (PDX) exhibit resistance to PI3K inhibitors due to a feedback upregulation of E6 and E7. The clinical relevance of this adaptive response is underscored by the finding that upregulation of E6 and E7 is mediated by HER3, which can be therapeutically targeted to enhance the efficacy of PI3K inhibitors in HPV(+) tumors.

Materials and Methods

Cell lines

The HPV(+) HNSCC cell lines UM-SCC47, 93-VU-147T, UPCI-SCC90, UD-SCC2, and UM-SCC104 were kindly provided by Dr. Randall Kimple (University of Wisconsin-Madison, Madison, WI). The HPV(+) HNSCC cell line UPCI-SCC152 was purchased from ATCC. All HPV(+) cell lines were maintained in DMEM with 10% FBS (Gemini Bio-Products) and 1% penicillin and streptomycin (Life Technologies) supplemented with 1% nonessential amino acids (Gibco). The HPV(−) cell lines SCC9 and Detroit562 were purchased from ATCC. PE/CA-PJ49 and PE/CA-PJ34 (clone 12) were purchased from Sigma-Aldrich. CAL33 was kindly provided by Dr. Gerard Milano (University of Nice, Nice, France). HSC-2 was obtained from the Health Science Research Resources Bank (Osaka, Japan). UM-SCC4, UM-SCC1, and TU138 were kindly provided by Thomas E. Carey (University of Michigan, Ann Arbor, MI). Normal oral keratinocytes-spontaneously immortalized (NOKSI) were kindly provided by Dr. Silvio Gutkind (University of California, San Diego, San Diego, CA). All HPV(−) cell lines were maintained in DMEM with 10% FBS and 1% penicillin and streptomycin. NOKSI cells were maintained in Keratinocyte SFM and supplemented with defined keratinocyte-SFM growth supplement (Gibco). CAL33, HSC-2, and Detroit562 express mutant *PIK3CA* (H1047R). All cell lines were authenticated by short tandem repeat testing (Genetica DNA Laboratories).

Antibodies and chemical compounds

All antibodies used are indicated below: HER3-XP, p-HER3-Y1197, p-AKT-S473, p-AKT-T308, AKT, p-rpS6-S235/236, rpS6, p-p70S6K-T308, p70S6K, and GAPDH (Cell Signaling Technology), b-Tubulin (Abcam), E6 (2E-3F8; Euromedex), E7 (Invitrogen), E7, horseradish peroxidase (HRP)-conjugated goat-antirabbit IgG, and goat-anti-mouse IgG (Santa Cruz Biotechnology Inc). A combination of both E7 antibodies (1:1) was used for immunoblotting. E6 and E7 antibodies were diluted 1:500 in SuperBlock Buffer (Thermo Fisher Scientific).

The PI3K-targeted therapies BYL719, BKM120, and BEZ235 were purchased from Selleckchem (www.Selleckchem.com). All compounds were dissolved in DMSO for *in vitro*

experiments. CDX-3379 and the control IgG1 antibody CDX-0062C, were kindly provided by Celldex Therapeutics under a Material Transfer Agreement.

Plasmids, transfection, and establishment of stable cell lines

HPV16-E6 and HPV16-E7 were cloned into the doxycycline-inducible pLVX-Puro vector (Clontech) using the gateway cloning system (Life Technologies). pDONR223-ERBB3 was a kind gift from Drs. William Hahn (Dana Farber/Harvard Cancer Institute, Boston, MA) and David Root (Addgene plasmid #23874; ref. 32) and was subsequently cloned into pLX302 using the gateway system; pLX302 was a gift from David Root (Broad Institute, Cambridge, MA; Addgene plasmid #25896; ref. 33). All vectors were sequence validated. Lentivirus was produced according to the Lenti-X Tet-One Inducible Expression Systems Manual (Clontech) and subsequently used to establish TU138, 93-VU-147T, and UPCI-SCC90 stable cell lines after selection with puromycin (0.5 μg/mL) for several weeks. Validation of TU138-stable clones was performed 48 hours after incubation with doxycycline (1 μg/mL) and subsequently examined by qPCR for E6 and E7 expression. Validation for HER3 overexpression was examined by immunoblot analysis.

siRNA and transfection

For siRNA-mediated silencing, cells were transiently transfected with siRNAs targeting E6 and E7 (Santa Cruz Biotechnology, sc-156008 and sc-270423), HER3 siRNA (ON-TARGETplus, SMARTpool #L-003127; GE Dharmacon) or nontargeting siRNA (siNT; ON-TARGETplus Non-targeting Pool, #D-001810; Dharmacon). Lipofectamine RNAiMAX was used for all siRNA experiments according to the manufacturer's instructions (Life Technologies).

Cellular proliferation assay and determination of IC_{50}

Cells were seeded in 96-well plates at 30%−50% confluency and treated with escalating concentrations of BYL719, BKM120, or BEZ235 (0–20 μmol/L). After 72 hours of treatment with corresponding drug or siRNA transfection, cells were washed with PBS and fixed/stained with 0.5% crystal violet diluted in methanol. Plates were air dried overnight and dye was eluted with 0.1 mol/L sodium citrate (pH 6.0) diluted in 50% ethanol. After brief agitation, the absorbance was measured at 595 nm (A595) to determine cell growth. The percentage cell proliferation was calculated by comparison of the A595 reading from drug-treated or siRNA-transfected cells versus control cells. IC_{50} values were calculated with GraphPad Prism (GraphPad Software).

Fractional product method for drug combination synergy

The nature of the interaction between BYL719 or BKM120 and the HER3 antagonist CDX-3379 was evaluated via the fractional product method described by Chou and Talalay (34). Briefly, this method utilizes the relative cell density following treatment with each individual agent and calculates the expected (E) effect of combination therapy as a product of the individual responses. The observed (O) effect is the relative cell density following dual treatment. A ratio of the observed to expected (O:E) values was calculated and used to

estimate the synergy, additivity, or antagonism. A value less than 1 indicated synergism, greater than 1 demonstrated antagonism, and 1 represented additivity.

Apoptosis assay

HNSCC cells were plated in 6-well dishes and treated with vehicle, BYL719, or BKM120 for 72 hours. Alternatively, HNSCC cells were transfected with nontargeting siRNA (siNT) or siE6E7 and treated with BYL719 for 72 hours. Cells were then harvested with 0.5% trypsin, washed with PBS, and resuspended in 100 μL of binding buffer (BD Biosciences). Cells were stained with 2 mL of FITC-conjugated Annexin-V antibody and 2 μL of propidium iodide (FITC Annexin-V Apoptosis Detection Kit, BD Biosciences). The cells were analyzed by flow cytometry (Calibur DxP8). FlowJo Software (Tree Star, Inc.) was used to analyze the data.

Immunoblotting

Whole-cell lysates were harvested using RIPA lysis buffer (50 mmol/L Tris-HCl pH7.5, 150 mmol/L NaCl, 0.1% SDS, 0.5% deoxycholate, 0.5% NP-40) supplemented with protease inhibitor cocktail (Sigma P8340) and phosphatase inhibitor cocktails 2 and 3 (Sigma P5726 and P0044) on wet ice. Samples were sonicated for 10 seconds and then centrifuged at 15,000 × *g* for 10 minutes at 4° C. Bradford assay was used to determine protein concentrations (Bio-Rad Laboratories). Equal amounts of protein were fractionated by SDS-PAGE, transferred to a poly-vinylidene fluoride membrane (Bio-Rad Laboratories), and analyzed by incubation with the appropriate primary antibody. Proteins were detected via incubation with HRP-conjugated secondary antibodies and ECL Western Blotting Substrate (Santa Cruz Biotechnology) or SuperSignal West Femto Maximum Sensitivity Chemiluminescent Substrate (Thermo Fisher Scientific).

cDNA synthesis and quantitative PCR

Total RNA was isolated using RNeasy kit purchased from Qiagen. One microgram of total RNA was used to make cDNA using the iScript Reverse Transcription Supermix Kit (Bio-Rad Laboratories). qRT-PCR was conducted using CFX96 Touch Real-Time PCR Detection System (Bio-Rad). All reactions were performed in triplicate and repeated three times. To determine the normalized value, $2^{\Delta\Delta C_t}$ values were compared between E6 or E7 and β-Actin, where the change in crossing threshold (ΔC_t) = $C_{t\ \text{Target}} - C_t$ Control and $\Delta\Delta C_t = \Delta C_{t\ (\text{Vector})} - \Delta C_{t\ (\text{Stable Clone})}$. The sequences of primer sets used for this analysis are; E6-F: 5′-CTGCAATGTTTCAGGACCCA-3′, E6-R: 5′ -TCATGTATAGTTGTTTGCAGCTCrGT-3′; E7-F: 5′ -ACCGGACAGAGCCCATTACA-3′, E7-R: 5′-GCCCATTAACAGGTCTTCCAAA-3′; β-Actin-F: 5′-CAGCCATGTACGTTGCTATCCAGG-3′, β-Actin-R: 5′-AGGTCCAGACGCAGGATGGCATG-3′.

Receptor tyrosine kinase profiling

Luminex PhosphoRTK bead array assays were conducted according to manufacturer's instructions (R&D Systems, custom kit). Briefly, cells cultured in 6-well plates were washed twice in ice-cold PBS then lysed with 100 μL of the supplied lysis buffer 15 supplemented

with protease and phosphatase inhibitor cocktails (Sigma). Protein extracts were diluted with diluent buffer RD2–3 and 25 μL, containing 6 μg of protein, was added to 25 μL bead-detection mixture in round-bottom nonbinding 96-well plates (Corning 3605). Plates were sealed and incubated overnight at 4°C. Luminex beads were collected on a 96-well magnet and washed twice with 75 μL of Luminex sheath fluid. Beads were resuspended in 60 μL of sheath fluid and analyzed using a Luminex 200 instrument.

Establishment of cell line and patient-derived xenografts

All animal procedures and maintenance were conducted in accordance with protocols approved by the Institutional Animal Care and Use Committee of the University of California, San Francisco (San Francisco, CA). HNSCC PDXs were established from patients with newly diagnosed or recurrent HNSCC upon written consent in accordance with Institutional Review Board approval as described previously (35). Female Hsd:athymic Nude-Foxn1^{nu} mice were injected bilaterally with UM-SCC47 cells (1×10^6 cells). HNSCC PDXs were established in female *NOD.Cg-Prkdc*^{scid}*Il2rg*^{tm1Wjt}*/SzJ* (NSG) mice as described previously (35). Once xenografts reached 100 mm^3 to 200 mm^3, mice were randomized into treatment groups and started on their respective treatments. The dose of BYL719 and BKM120 used was 20 mg/kg [diluted in 0.5% carboxymethylcellulose sodium salt (Sigma) in water] and were administered 5 days/week by oral gavage. The dose of CDX-3379 was 10 mg/kg and was administered biweekly by intraperitoneal injection. For all xenograft experiments examining tumor volume, animals were randomized into respective treatment groups with $n = 5–8$ tumors per group. For analysis of signaling parameters after 5 days of BYL719 treatment, $n = 4$ to 6 tumors per treatment group. All tumors were harvested 3 hours after the last treatment. Tumor volume measurements were determined by digital calipers biweekly and calculated using the formula $(\pi)/6 \times$ (large diameter) $\times$ (small diameter)^2. Tumor volumes for all xenograft experiments were calculated as fractions of the average starting volume for each group, and the mean tumor volume ± SEM is shown.

IHC

Extracted tumor tissue was collected at the indicated time periods, fixed in 10% neutral-buffered formalin, paraffin-embedded, and cut into sections. The sections were heated in 10 mmol/L citrate buffer (pH 6.0) for Ki67 or in EDTA buffer (pH 8.0) for HER3 and E7 in a decloaking chamber. Staining commenced using the Universal quick kit following the manufactures instructions (Vector Laboratories, Inc., PK-8800). Samples were incubated overnight at 4°C with the following antibodies: Ki67 (Cell Signaling Technology, 1:1,000), HER3 (Cell Signaling Technology, 1:50), and E7 (Santa Cruz Biotechnology, 1:50). Antibody binding was revealed by addition of 3,3′-diaminobenzidine substrate and counterstained with Mayer hematoxylin (Vector Laboratories). Tissues were examined using a Nikon Eclipse microscope and quantitation of staining intensity was performed with Figi software.

Statistical analysis

For all *in vitro* assays, at least three replicates were analyzed with the same experimental conditions, and at least three independent experiments were performed. Two-tailed Student t

test was used to evaluate differences in cell proliferation and apoptosis. Student t test was also used to evaluate differences in protein abundance in immunoblots and staining intensity for IHC images. For *in vivo* growth assays, 5 to 8 tumors per treatment group were analyzed. To evaluate the sensitivity of cell line xenografts or PDXs to the different therapies, the mean fractional tumor volumes were compared between the vehicle treated and drug treatment arms at the last time point of the study using two-sample *t* tests with equal SDs.

Results

HPV(+) HNSCC preclinical models are less sensitive to PI3K inhibitors than HPV(−) models

Because the PI3K pathway is commonly activated in HPV(+) tumors, we hypothesized that HPV(+) HNSCCs would be more sensitive to PI3K inhibitors than HPV(−) HNSCCs. To test this hypothesis, the antiproliferative effects of several different PI3K inhibitors were examined in a panel of HPV(+) and HPV(−) HNSCC cell lines (see Materials and Methods for molecular characteristics of cell lines examined). We first determined the half-maximal inhibitory concentration (IC_{50}) for BYL719 (a p110a-specific inhibitor that is currently in phase II clinical trials in HNSCC) in six HPV(+) and nine HPV(−) cell lines after 72 hours of treatment. The IC_{50} concentration for BYL719 in all HPV(+) cell lines tested ranged from 3.5 μmol/L to 15.0 μmol/L, whereas the IC_{50} concentration in HPV(−) cell lines ranged from 0.75 μmol/Lto 5.2 μmol/L (Fig. 1A). Furthermore, HPV(−) cell lines treated with 1.0 μmol/L BYL719 demonstrated significant increases in apoptosis relative to HPV(+) cells, as assessed by Annexin V staining (Fig. 1B). Collectively, HPV(+) cell lines were more resistant to BYL719 than were HPV(−) cell lines in both proliferation and apoptosis assays ($P = 0.004$ and $P = 0.03$, respectively; Fig. 1C). Similar results were seen with BKM120, a clinically advanced pan-PI3K inhibitor, and the dual PI3K/mTOR inhibitor BEZ235 (Supplementary Fig. S1).

To characterize the biochemical effects of BYL719 in HPV(+) and HPV(−) cell lines, PI3K pathway signaling was analyzed 72 hours after BYL719 treatment via immunoblotting for AKT and rpS6 (Fig. 1D). BYL719 did not abrogate phosphorylation of AKT-S473 or rpS6-S235/236 in the HPV(+) lines, whereas treatment with BYL719 markedly reduced phosphorylation of these proteins in HPV(−) cell lines (Fig. 1D). These data suggest that p110a inhibition does not effectively block signaling through AKT and rpS6 in HPV(+) cells, which may likely contribute to reduced sensitivity to PI3K inhibitors.

To extend these findings to more clinically relevant models, we examined the antitumor effects of PI3K inhibitors in HPV(+) and HPV(−) patient-derived xenografts (PDXs; see Supplementary Table S1 for clinical characteristics of the PDXs examined). Four HPV(+) and two HPV(−) PDXs were established in *NOD.Cg-Prkdc*^{scid}*Il2rg*^{tm1Wjt}*/SzJ* (NSG) mice and treated with BYL719 (20 mg/kg by oral gavage) for five consecutive days. In all four HPV(+) PDXs, including the HPV(+)/*PIK3CA*-mutant PDX (PDX-4), five-day treatment with BYL719 did not significantly reduce the percentage of Ki67-positive nuclei (Fig. 1E). In contrast, the two HPV(−) PDXs treated with BYL719 demonstrated significant reductions in Ki67-positive nuclei compared with vehicle-treated tumors. BYL719 reduced expression of phospho-AKT(S473) and phospho-rpS6(S235/236) in the HPV(−) PDX-5, while the phosphorylation of these proteins were only marginally reduced in HPV(+) PDXs (Fig. 1F).

To determine whether these findings were consistent among different PI3K inhibitors, the antitumor effects of the pan-PI3K inhibitor BKM120 were assessed in a representative HPV(+) PDX (PDX-3) and an HPV(−) PDX (PDX-5). Treatment with BKM120 for 21 days (20 mg/kg, 5 days/week by oral gavage) inhibited the growth of the HPV(−) PDX while exerting little effect on the HPV(+) PDX (Fig. 1G). Analysis of PI3K pathway signaling in tumors harvested after the last treatment indicated that phospho-AKT(S473) and phospho-rpS6(S235/236) were markedly reduced in BKM120-treated HPV(−) tumors, but only marginally reduced in HPV(+) tumors (Fig. 1H). Taken together, these results suggest that PI3K inhibitors may be ineffective as single-agent therapies in HPV(+) HNSCCs.

HPV16 E6 and E7 oncoproteins mediate resistance to PI3K inhibitors

Given our findings that HPV(+) HNSCC preclinical models were relatively resistant to PI3K-targeted therapies, we next explored the role of the E6 and E7 oncoproteins in mediating resistance. Proliferation assays were performed in three HPV(+) cell lines transfected with pooled siRNAs targeting polycistronic E6 and E7 RNAs followed by treatment with 1.0 μmol/L of BYL719 (Fig. 2A). Consistent with previous reports (36, 37), knockdown of E6 and E7 reduced the proliferation of all three HPV(+) cell lines. Immunoblot analysis confirmed the knockdown of E6 and E7 with the siRNAs used. Knockdown of E6 and E7 sensitized HPV(+) cell lines to BYL719 in proliferation assays (Fig. 2A). Furthermore, siRNA depletion of E6 and E7 increased BYL719-induced apoptosis in all three HPV(+) cell lines tested (Fig. 2B). The knockdown of E6 and E7 in combination with BYL719 also reduced phosphorylation of AKT(S473), p70S6-kinase(T389), and rpS6(S235/236) substantially more than E6 and E7 knockdown or BYL719 treatment alone in all HPV(+) lines tested (Fig. 2C).

To confirm the role for HPV oncoproteins in PI3K inhibitor resistance, E6 and E7 lentiviral particles were transduced into the HPV(−) cell line TU138 (Fig. 2D). Compared with vector-transduced control cells, two independent clones overexpressing E6 and E7 displayed increased PI3K pathway signaling, as indicated by enhanced phosphorylation of AKT(S473) and rpS6 (S235/236; Fig. 2D, right). Whereas vector-transduced cells were highly sensitive to 1.0 μmol/L BYL719 and BKM120, exogenous expression of E6 and E7 resulted in reduced sensitivity to both agents (by ~34%−45%; Fig. 2E). Furthermore, both BYL719 and BKM120 induced apoptosis in vector-transduced control cells, while E6- and E7-expressing clones were more resistant to BYL719- and BKM120-induced apoptosis (by ~20%; Fig. 2F). Overall, these findings suggest that E6 and E7 can promote resistance to PI3K inhibitors in HPV-associated HNSCCs.

PI3K inhibitors activate the HER3/AKT signaling pathway in HPV(+) HNSCC preclinical models

We next sought to elucidate the molecular mechanism by which HPV oncoproteins might contribute to PI3K inhibitor resistance. We recently reported that E6 and E7 induce expression of HER3 in HPV(+) HNSCC models (25). HER3 has also been implicated in resistance to PI3K inhibitors in breast cancer (38–40). To determine whether HER3 mediates resistance to PI3K inhibitors in HPV(+) HNSCC, we analyzed the phosphorylation status and total abundance of HER3 over a 24-hour time course of BYL719 treatment (Fig. 3A).

Within 8 hours of BYL719 exposure, HER3 and phospho-HER3 (Y1197) protein levels were increased in HPV(+) cell lines UM-SCC47 and 93-VU-147T. This time course also revealed that phosphorylation of AKT, at both serine 473 and threonine 308, was reduced by 15 minutes but was restored within 24 hours of treatment. In the HPV(+) cell line SCC90, HER3 and phospho-HER3 protein levels were increased within 15 minutes of BYL719 exposure, and no detectable change in AKT phosphorylation was observed. A phospho-RTK screen was also performed in HPV(+) cell lines treated with 1.0 μmol/L of BYL719 for 24 hours. The results indicated that HER3 was the only RTK whose phosphorylation increased in all three HPV(+) cell lines following treatment with BYL719 (Supplementary Fig. S2). In contrast to HPV(+) cell lines, HER3 protein levels were either unchanged or reduced in all three HPV(−) cell lines treated with BYL719, and AKT phosphorylation was inhibited up to 24 hours (Fig. 3A). Feedback signaling through HER3/AKT was also observed in HPV(+) cell lines treated with BKM120 and BEZ235 over a 24-hour time course (Supplementary Fig. S3).

As total HER3 was increased in HPV(+) cell lines treated with PI3K inhibitors, we next determined whether this was reflected in expression of HER3 on the plasma membrane (Fig. 3B). Flow cytometric analysis demonstrated a significant increase in HER3 surface levels in HPV(+) cell lines treated with BYL719. We then tested the hypothesis that the reactivation of AKT observed after PI3K inhibitor treatment is dependent on HER3. HPV(+) cell lines were transfected with siRNA targeting HER3 or a nontargeting control (siNT) for 48 hours followed by treatment with BYL719 for up to 24 hours (Fig. 3C). While AKT was reactivated within 8 hours of BYL719 exposure in cells transfected with siNT, reactivation was either reduced or blocked in cells depleted of HER3.

To determine whether similar mechanisms occur in HPV(+) *in vivo* models, we evaluated the abundance and phosphorylation status of HER3 in HPV(+) PDXs treated with BYL719 for five consecutive days (Fig. 3D). Analysis of tumors harvested from three HPV(+) PDXs (PDX-1, PDX-2, and PDX-3) indicated that HER3 phosphorylation and abundance were increased in tumors after five days of BYL719 treatment. IHC staining also demonstrated strong HER3 staining on the plasma membrane in BYL719-treated tumors (Fig. 3E). Collectively, these results suggest that the HER3/AKT signaling pathway is activated in HPV(+) preclinical models in response to PI3K inhibitor treatment.

HER3 regulates the abundance of E6 and E7 in HPV(+) predinical models

Our data indicate that HPV E6 and E7 oncoproteins promote resistance to PI3K inhibitors in HPV(+) models and that HER3/AKT signaling is rapidly activated following PI3K inhibition. We next sought to determine the impact of HER3 signaling on E6 and E7 expression. Similar to HER3, E6 and E7 protein levels were increased in HPV(+) cell lines treated with BYL719 for 24 hours (Fig. 4A). To determine whether this increase in E6 and E7 was dependent on HER3, HER3 expression was knocked down using siRNA and then E6 and E7 protein levels were analyzed. Downregulation of HER3 resulted in reduced E6 and E7 protein levels (Fig. 4B). Conversely, ectopic overexpression of HER3 in the HPV(+) cell lines 93-VU-147T and UPCI-SCC90 led to increased E6 and E7 protein levels compared

with vector-transduced control cells (Fig. 4C). Importantly, HER3 down-regulation prevented increases in E6 and E7 oncoproteins following BYL719 treatment (Fig. 4D).

To extend these *in vitro* studies to our *in vivo* models, E6 and E7 protein levels were analyzed in HPV(+) PDXs treated with BYL719 for five days. As observed with HER3, BYL719 treatment led to increased abundance of E6 and E7 in three HPV(+) PDXs treated with BYL719 (Fig. 4E). IHC staining for E7 confirmed this result in HPV(+) PDX-1, in which more robust nuclear E7 staining was observed in BYL719-treated tumors (Fig. 4F). Together, these data suggest that cross-talk between HER3 and HPV oncoproteins is increased in HPV(+) preclinical models treated with PI3K inhibitors.

Targeting HER3 enhances the efficacy of PI3K inhibitors and sustains knockdown of the PI3K pathway

As cross-talk between HER3 and HPV oncoproteins was elevated in PI3K inhibitor-treated cells, we hypothesized that suppression of HER3 signaling would reduce the abundance of E6 and E7 and sensitize HPV(+) preclinical models to PI3K inhibitors. To test this hypothesis, proliferation assays were performed in HPV(+) cell lines after suppressing HER3 expression with siRNA and treating with BYL719 (Fig. 5A). The combination of HER3 siRNA and BYL719 reduced the proliferation of three HPV (+) cell lines more robustly than single-agent BYL719 or siHER3 alone. Similar results were observed in HPV(+) cell lines depleted of HER3 and treated with BKM120 (Supplementary Fig. S4A). Next, the anti-HER3 mAb CDX-3379, which is in active clinical development in HNSCC, was tested in combination with BYL719. CDX-3379 locks HER3 in an inactive conformation, inhibiting both ligand-dependent and -independent activation of HER3 (41). In proliferation assays, CDX-3379 significantly enhanced the efficacy of BYL719in all HPV(+) cell lines examined (Fig. 5B). Although HPV(−) cell lines were sensitive to BYL719, CDX-3379 did not enhance this effect. The combination of CDX-3379 and BYL719 was evaluated for synergy using the fractional product method described by Chou and Talalay (34). HER3 inhibition synergized with BYL719 in each of the HPV(+) cell lines examined (Fig. 5B). CDX-3379 was also found to synergize with BKM120 in HPV(+) cell lines (Supplementary Fig. S4B). Immunoblot analysis indicated that the combination of CDX-3379 and BYL719 suppressed the phosphorylation of AKT and rpS6 more than either treatment alone (Fig. 5C). Furthermore, targeting HER3 with CDX-3379 reduced E6 and E7 levels and prevented their upregulation by BYL719 (Fig. 5C). Together, these results demonstrate that targeting HER3 can enhance the efficacy of PI3K inhibitors and sustain knockdown of the PI3K pathway in HPV (+) cells.

Targeting HER3 overcomes PI3K inhibitor resistance in HPV(+) xenografts

We next assessed the impact of HER3 inhibition on response to BYL719 *in vivo.* The HPV(+) cell line UM-SCC47 and two HPV(+) PDXs, PDX-1 and PDX-4, were established in athymic nude or NSG mice (Fig. 6A). Tumor-bearing mice were treated with vehicle, BYL719 (20 mg/kg), CDX-3379 (10 mg/kg), or the combination for 19–22 days (n = 5–8 tumors per treatment group; Fig. 6A). While UM-SCC47 tumors were moderately sensitive to BYL719, PDX-1 and PDX-4 exhibited only a minor response to BYL719. All the xenograft models responded to CDX-3379, but the combination of BYL719 and CDX-3379

was significantly more potent than single-agent CDX-3379 therapy (Fig. 6A). Tumors from mice bearing PDX-1 were harvested at the end of the study to analyze PI3K pathway signaling (Fig. 6B). Expression of total and phosphorylated HER3 was increased in tumors treated with BYL719, but reduced in tumors treated with CDX-3379. Compared with single-agent treatment groups, tumors harvested from the combination group had reduced levels of phospho-AKT, phospho-rpS6, and nuclear Ki67 (Fig. 6C and D). Consistent with results in HPV(+) cell lines, IHC revealed robust staining for HER3 and E7 in BYL719-treated PDX-1, while CDX-3379 reduced the staining intensity of both proteins. Taken together, these data demonstrate that cotargeting HER3 and PI3K can overcome PI3K inhibitor resistance and block feedback signaling through HER3 and E7 *in vivo*.

Discussion

PI3K-targeted therapies are currently in clinical development for the treatment of HNSCC. Initial results have shown only moderate clinical benefit in unselected patient populations with the rapid emergence of drug resistance (42, 43). As the PI3K pathway is activated in HPV(+) HNSCCs, we hypothesized that HPV(+) preclinical models would be sensitive to PI3K-targeting strategies. Contrary to our original hypothesis, we found that HPV(+) HNSCC models were more resistant to PI3K inhibitors than HPV(−) models. PI3K inhibitor resistance was attributed to feedback signaling emanating from HER3 and HPV oncoproteins, which maintained AKT activity in PI3K inhibitor-treated cells. Blocking HER3 activity abrogated this feedback loop and enhanced the efficacy of PI3K inhibitors. This is the first study to identify a role for HPV oncoproteins in HNSCC drug resistance and provides a rational cotargeting strategy to improve the efficacy of PI3K inhibitors in HPV(+) tumors.

Our results demonstrated that HPV(+) HNSCC cell lines and PDXs were less responsive to PI3K inhibitors than HPV(−) models. This difference in drug sensitivity may be attributed to the reactivation of AKT by HER3 following PI3K inhibitor treatment of HPV(+) cells. Suppression of HER3 reduced this adaptive response and enhanced the efficacy of PI3K inhibitors in HPV(+) cell line and tumor models. A similar observation was reported in preclinical models of HER2(+) breast cancer, in which PI3K inhibition resulted in FoxO1-dependent upregulation of HER3 and reactivation of AKT following treatment (38). Others reported that the RTK AXL mediates acquired resistance to PI3Ka inhibition independent from AKT reactivation in HPV(−) *PIK3CA*-mutant HNSCC models (44). Consistent with these findings, PI3K inhibitors blocked AKT signaling in HPV(−) HNSCC cell lines and PDXs tested in the current study, and these cell lines were relatively sensitive to PI3K inhibitors in short-term assays. In contrast to the current findings, previous studies demonstrated that UD-SCC2 and UM-SCC47 cells were relatively sensitive to the mTOR inhibitors rapamycin and RAD001 (30, 45). Both inhibitors reduced the phosphorylation of AKT and rpS6 in these models (30, 45). This discrepancy in results may be due to differences in feedback signaling cascades that are activated upon inhibition of different nodes of the PI3K pathway. Further research is necessary to determine the most effective way of suppressing PI3K/AKT signaling in HPV(+) HNSCCs. Taken together, the reactivation of AKT by HER3 may limit the efficacy of PI3K inhibitors in HPV(+)

HNSCCs, and therefore cotargeting HER3 and PI3K may be an effective therapeutic strategy to overcome PI3K inhibitor-resistance in HPV(+) tumors.

E6 and E7 are ubiquitously expressed in HPV(+) tumors, where integration of viral DNA into the host's genome results in stabilization and heightened expression of E6 and E7 in the tumor (1, 46, 47). One of the consequences of E6 and E7 expression is increased stabilization of, and signaling through, RTKs (21, 22). Our results show that HER3 can reciprocally increase the abundance of E6 and E7 in HPV(+) cells. Cross-talk between HER3 and HPV oncoproteins was heightened in PI3K inhibitor-treated cells, resulting in maintenance of AKT activity and PI3K inhibitor resistance. This mechanism of PI3K inhibitor resistance is supported by the finding that knockdown of E6 and E7, or blockade of HER3, sensitized HPV(+) cells to PI3K inhibitors. To our knowledge, this is the first study to report reciprocal feedback signaling between an RTK and HPV oncoproteins. This finding suggests that therapeutic targeting of HER3 could be a novel method to decrease the abundance of E6 and E7 in HPV(+) tumors. The precise mechanism underlying HER3 upregulation of E6 and E7 remains incompletely understood; however, we speculate that HER3-mediated activation of AKT could play an important role. Collectively, these data highlight a new adaptive response to PI3K inhibitors that may limit the efficacy of these agents in HPV(+) tumors.

While HPV oncoproteins activate the PI3K pathway in HPV(+) tumors, *PIK3CA* mutation and/or amplification can also contribute to hyperactivation of the pathway. Several preclinical studies and early-phase clinical trials suggest that *PIK3CA* mutation is correlated with increased response to PI3K pathway inhibitors (48–50). However, other studies have shown no consistent correlation between *PIK3CA* mutation status and enhanced response to PI3K-targeted therapies (42, 43, 51, 52). In the current study, HPV(+) PIK3CA-mutant and wild-type PDXs were less sensitive to PI3K inhibitors than HPV(−) PDXs. While these data suggest that HPV(+) tumors may be intrinsically resistant to PI3K inhibitors irrespective of *PIK3CA* mutation status, the paucity of HPV(+)/PIK3CA-mutant HNSCC cell lines limits our ability to fully test this hypothesis in cell culture models. To date, only a small panel of HPV(+) HNSCC cell lines have been generated, and all express wild-type *PIK3CA.* Furthermore, HPV(−) *PIK3CA*-mutant and wild-type HNSCC cell lines were found to be sensitive to PI3K inhibitors, suggesting that additional biomarkers beyond *PIK3CA* mutation are needed to more broadly identify PI3K inhibitor-responsive tumors.

Targeting HER3 reversed PI3K inhibitor resistance in HPV(+) HNSCC cell lines and PDXs. This finding is in accordance with several preclinical studies demonstrating robust antitumor effects of cotargeting PI3K with RTKs in different tumor models (38, 40, 44). The challenge in moving this strategy into clinical trials will be to predict which RTK to target based on the molecular and genetic underpinnings of each patient's tumor, in addition to managing the likely toxicities of combined approaches. Our recent work demonstrates that HER3 is overexpressed and active in HPV(+) HNSCCs (25, 53), suggesting that HER3 could be an important molecular target in HPV(+) tumors. In comparison with HPV(+) preclinical models, the HPV(−) cell lines tested did not respond to the dual targeting of HER3 and PI3K. Thus, HPV(−) tumors may benefit from alternative cotargeting strategies to enhance responses to PI3K inhibitors. The feasibility of the proposed cotargeting approach is further

supported by a recent phase Ib clinical trial demonstrating that the combination of a HER3 antagonist with a PI3K inhibitor was safe and well tolerated by breast cancer patients (54).

In summary, this study suggests that cross-talk between HER3 and HPV oncoproteins maintains signaling through AKT in HPV(+) tumors treated with PI3K inhibitors. We propose that this mechanism could limit the clinical efficacy of PI3K inhibitors in HPV(+) patients. As a result, combined blockade of HER3 and PI3K may prevent this feedback resistance mechanism and be an effective therapeutic strategy for the treatment of patients with HPV(+) HNSCC.

Supplementary Material

Refer to Web version on PubMed Central for supplementary material.

Acknowledgments

The authors thank Dr. Danielle Swaney (University of California, San Francisco, San Francisco, CA) for critically reviewing this manuscript. The project described was supported by RO1 DE023685 from the National Cancer Institute (to J. Grandis), the American Cancer Society (to J. Grandis), the V Foundation for Cancer Research (to J.E. Bauman), Career Development Award CDA-2-057-10S from the Department of Veterans Affairs (to U. Duvvuri), grant Z-2/59 from the Interdisciplinary Center for Clinical Research of the University Würzburg (to S. Hartmann), postdoctoral fellowship PF-16-087-01-TBG from the American Cancer Society (to T.M. Brand), by NIH grant T32 CA108462 for Molecular and Cellular Mechanisms of Disease (to T.M. Brand), and U54 CA209891 (to N.J. Krogan).

The costs of publication of this article were defrayed in part by the payment of page charges. This article must therefore be hereby marked *advertisement* in accordance with 18 U.S.C. Section 1734 solely to indicate this fact.

References

1. Moody CA, Laimins LA. Human papillomavirus oncoproteins: pathways to transformation. Nat Rev Cancer 2010;10:550–60. [PubMed: 20592731]
2. Bodily J, Laimins LA. Persistence of human papillomavirus infection: keys to malignant progression. Trends Microbiol 2011;19:33–9. [PubMed: 21050765]
3. Chung CH, Bagheri A, D'Souza G. Epidemiology of oral human papillomavirus infection. Oral Oncol 2014;50:364–9. [PubMed: 24080455]
4. Kang H, Kiess A, Chung CH. Emerging biomarkers in head and neck cancer in the era of genomics. Nat Rev Clin Oncol 2015;12:11–26. [PubMed: 25403939]
5. Chaturvedi AK, Engels EA, Pfeiffer RM, Hernandez BY, Xiao W, Kim E, et al. Human papillomavirus and rising oropharyngeal cancer incidence in the United States. J Clin Oncol 2011;29:4294–301. [PubMed: 21969503]
6. Ang KK, Harris J, Wheeler R, Weber R, Rosenthal DI, Nguyen-Tan PF, et al. Human papillomavirus and survival of patients with oropharyngeal cancer. N Engl J Med 2010;363:24–35. [PubMed: 20530316]
7. Fakhry C, Westra WH, Li S, Cmelak A, Ridge JA, Pinto H, et al. Improved survival of patients with human papillomavirus-positive head and neck squamous cell carcinoma in a prospective clinical trial. J Natl Cancer Inst 2008;100:261–9. [PubMed: 18270337]
8. Trosman SJ, Koyfman SA, Ward MC, Al-Khudari S, Nwizu T, Greskovich JF, et al. Effect of human papillomavirus on patterns of distant metastatic failure in oropharyngeal squamous cell carcinoma treated with chemoradiotherapy. JAMA Otolaryngol Head Neck Surg 2015;141:457–62. [PubMed: 25742025]
9. Ragin CC, Taioli E. Survival of squamous cell carcinoma of the head and neck in relation to human papillomavirus infection: review and metaanalysis. Int J Cancer 2007;121:1813–20. [PubMed: 17546592]

10. Munger K, Phelps WC, Bubb V, Howley PM, Schlegel R. The E6 and E7 genes of the human papillomavirus type 16 together are necessary and sufficient for transformation of primary human keratinocytes. J Virol 1989; 63:4417–21. [PubMed: 2476573]
11. Rampias T, Sasaki C, Psyrri A. Molecular mechanisms of HPV induced carcinogenesis in head and neck. Oral Oncol 2014;50:356–63. [PubMed: 23953776]
12. Jabbar S, Strati K, Shin MK, Pitot HC, Lambert PF. Human papillomavirus type 16 E6 and E7 oncoproteins act synergistically to cause head and neck cancer in mice. Virology 2010;407:60–7. [PubMed: 20797753]
13. McLaughlin-Drubin ME, Munger K. Oncogenic activities of human papillomaviruses. Virus Res 2009;143:195–208. [PubMed: 19540281]
14. Scheffner M, Werness BA, Huibregtse JM, Levine AJ, Howley PM. The E6 oncoprotein encoded by human papillomavirus types 16 and 18 promotes the degradation of p53. Cell 1990;63:1129–36. [PubMed: 2175676]
15. Dyson N, Howley PM, Munger K, Harlow E. The human papilloma virus- 16 E7 oncoprotein is able to bind to the retinoblastoma gene product. Science 1989;243:934–7. [PubMed: 2537532]
16. Vivanco I, Sawyers CL. The phosphatidylinositol 3-Kinase AKT pathway in human cancer. Nat Rev Cancer 2002;2:489–501. [PubMed: 12094235]
17. Menges CW, Baglia LA, Lapoint R, McCance DJ. Human papillomavirus type 16 E7 up-regulates AKT activity through the retinoblastoma protein. Cancer Res 2006;66:5555–9. [PubMed: 16740689]
18. Yarbrough WG, Whigham A, Brown B, Roach M, Slebos R. Phosphoinositide kinase-3 status associated with presence or absence of human papillomavirus in head and neck squamous cell carcinomas. Int J Radiat Oncol Biol Phys 2007;69(2 Suppl):S98–101. [PubMed: 17848307]
19. Spangle JM, Munger K. The human papillomavirus type 16 E6 oncoprotein activates mTORC1 signaling and increases protein synthesis. J Virol 2010; 84:9398–407. [PubMed: 20631133]
20. Surviladze Z, Sterk RT, DeHaro SA, Ozbun MA. Cellular entry of human papillomavirus type 16 involves activation of the phosphatidylinositol 3-kinase/Akt/mTOR pathway and inhibition of autophagy. J Virol 2013; 87:2508–17. [PubMed: 23255786]
21. Narisawa-Saito M, Handa K, Yugawa T, Ohno S, Fujita M, Kiyono T. HPV16 E6-mediated stabilization of ErbB2 in neoplastic transformation of human cervical keratinocytes. Oncogene 2007;26:2988–96. [PubMed: 17146442]
22. Spangle JM, Munger K. The HPV16 E6 oncoprotein causes prolonged receptor protein tyrosine kinase signaling and enhances internalization of phosphorylated receptor species. PLoS Pathog 2013; 9:e1003237. [PubMed: 23516367]
23. Akerman GS, Tolleson WH, Brown KL, Zyzak LL, Mourateva E, Engin TS, et al. Human papillomavirus type 16 E6 and E7 cooperate to increase epidermal growth factor receptor (EGFR) mRNA levels, overcoming mechanisms by which excessive EGFR signaling shortens the life span of normal human keratinocytes. Cancer Res 2001;61:3837–43. [PubMed: 11325860]
24. Paolini F, Curzio G, Melucci E, Terrenato I, Antoniani B, Carosi M, et al. Human papillomavirus 16 E2 interacts with neuregulin receptor degradation protein 1 affecting ErbB-3 expression in vitro and in clinical samples of cervical lesions. Eur J Cancer 2016;58:52–61. [PubMed: 26963794]
25. Brand TM, Hartmann S, Bhola NE, Peyser ND, Li H, Zeng Y, et al. Human papillomavirus regulates HER3 expression in head and neck cancer: implications for targeted HER3 therapy in HPV(+) patients. Clin Cancer Res 2017;23:3072–83. [PubMed: 27986750]
26. Pim D, Massimi P, Dilworth SM, Banks L. Activation of the protein kinase B pathway by the HPV-16 E7 oncoprotein occurs through a mechanism involving interaction with PP2A. Oncogene 2005;24:7830–8. [PubMed: 16044149]
27. Spanos WC, Hoover A, Harris GF, Wu S, Strand GL, Anderson ME, et al. The PDZ binding motif of human papillomavirus type 16 E6 induces PTPN13 loss, which allows anchorage-independent growth and synergizes with ras for invasive growth. J Virol 2008;82:2493–500. [PubMed: 18160445]
28. Tung MC, Lin PL, Cheng YW, Wu DW, Yeh SD, Chen CY, et al. Reduction of microRNA-184 by E6 oncoprotein confers cisplatin resistance in lung cancer via increasing Bcl-2. Oncotarget 2016;7:32362–74. [PubMed: 27083050]

29. McKenna DJ, Patel D, McCance DJ. miR-24 and miR-205 expression is dependent on HPV onco-protein expression in keratinocytes. Virology 2014;448:210–6. [PubMed: 24314651]
30. Molinolo AA, Marsh C, El Dinali M, Gangane N, Jennison K, Hewitt S, et al. mTOR as a molecular target in HPV-associated oral and cervical squamous carcinomas. Clin Cancer Res 2012;18:2558–68. [PubMed: 22409888]
31. Cancer Genome Atlas Network. Comprehensive genomic characterization of head and neck squamous cell carcinomas. Nature 2015;517: 576–82. [PubMed: 25631445]
32. Johannessen CM, Boehm JS, Kim SY, Thomas SR, Wardwell L, Johnson LA, et al. COT drives resistance to RAF inhibition through MAP kinase pathway reactivation. Nature 2010;468:968–72. [PubMed: 21107320]
33. Yang X, Boehm JS, Yang X, Salehi-Ashtiani K, Hao T, Shen Y, et al. A public genome-scale lentiviral expression library of human ORFs. Nat Methods 2011;8:659–61. [PubMed: 21706014]
34. Chou TC. Drug combination studies and their synergy quantification using the Chou-Talalay method. Cancer Res 2010;70:440–6. [PubMed: 20068163]
35. Li H, Wheeler S, Park Y, Ju Z, Thomas SM, Fichera M, et al. Proteomic characterization of head and neck cancer patient-derived xenografts. Mol Cancer Res 2016;14:278–86. [PubMed: 26685214]
36. Rampias T, Sasaki C, Weinberger P, Psyrri A. E6 and e7 gene silencing and transformed phenotype of human papillomavirus 16-positive oropharyngeal cancer cells. J Natl Cancer Inst 2009;101:412–23. [PubMed: 19276448]
37. Adhim Z, Otsuki N, Kitamoto J, Morishita N, Kawabata M, Shirakawa T, et al. Gene silencing with siRNA targeting E6/E7 as a therapeutic intervention against head and neck cancer-containing HPV16 cell lines. Acta Otolaryngol 2013;133:761–71. [PubMed: 23638950]
38. Chakrabarty A, Sanchez V, Kuba MG, Rinehart C, Arteaga CL. Feedback upregulation of HER3 (ErbB3) expression and activity attenuates antitumor effect of PI3K inhibitors. Proc Natl Acad Sci U S A 2012;109: 2718–23. [PubMed: 21368164]
39. Serra V, Scaltriti M, Prudkin L, Eichhorn PJ, Ibrahim YH, Chandarlapaty S, et al. PI3K inhibition results in enhanced HER signaling and acquired ERK dependency in HER2-overexpressing breast cancer. Oncogene 2011;30: 2547–57. [PubMed: 21278786]
40. Tao JJ, Castel P, Radosevic-Robin N, Elkabets M, Auricchio N, Aceto N, et al. Antagonism of EGFR and HER3 enhances the response to inhibitors of the PI3K-Akt pathway in triple-negative breast cancer. Sci Signal 2014;7:ra29. [PubMed: 24667376]
41. Xiao Z, Carrasco RA, Schifferli K, Kinneer K, Tammali R, Chen H, et al. A potent HER3 monoclonal antibody that blocks both ligand-dependent and -independent activities: differential impacts of PTEN status on tumor response. Mol Cancer Ther 2016;15:689–701. [PubMed: 26880266]
42. Jimeno A, Bauman JE, Weissman C, Adkins D, Schnadig I, Beauregard P, et al. A randomized, phase 2 trial of docetaxel with or without PX-866, an irreversible oral phosphatidylinositol 3-kinase inhibitor, in patients with relapsed or metastatic head and neck squamous cell cancer. Oral Oncol 2015;51:383–8. [PubMed: 25593016]
43. Rodon J, Brana I, Siu LL, De Jonge MJ, Homji N, Mills D, et al. Phase I dose-escalation and -expansion study of buparlisib (BKM120), an oral pan-Class I PI3K inhibitor, in patients with advanced solid tumors. Invest New Drugs 2014;32:670–81. [PubMed: 24652201]
44. Elkabets M, Pazarentzos E, Juric D, Sheng Q, Pelossof RA, Brook S, et al. AXL mediates resistance to PI3Kalpha inhibition by activating the EGFR/PKC/mTOR axis in head and neck and esophageal squamous cell carcinomas. Cancer Cell 2015;27:533–46. [PubMed: 25873175]
45. Madera D, Vitale-Cross L, Martin D, Schneider A, Molinolo AA, Gangane N, et al. Prevention of tumor growth driven by PIK3CA and HPV oncogenes by targeting mTOR signaling with metformin in oral squamous carcinomas expressing OCT3. Cancer Prev Res (Phila) 2015;8:197–207. [PubMed: 25681087]
46. Nakagawa S, Yoshikawa H, Yasugi T, Kimura M, Kawana K, Matsumoto K, et al. Ubiquitous presence of E6 and E7 transcripts in human papillomavirus-positive cervical carcinomas regardless of its type. J Med Virol 2000;62:251–8. [PubMed: 11002256]

47. Parfenov M, Pedamallu CS, Gehlenborg N, Freeman SS, Danilova L, Bristow CA, et al. Characterization of HPV and host genome interactions in primary head and neck cancers. Proc Natl Acad Sci U S A 2014;111: 15544–9. [PubMed: 25313082]

48. Janku F, Wheler JJ, Westin SN, Moulder SL, Naing A, Tsimberidou AM, et al. PI3K/AKT/mTOR inhibitors in patients with breast and gynecologic malignancies harboring PIK3CA mutations. J Clin Oncol 2012;30:777–82. [PubMed: 22271473]

49. O'Brien C, Wallin JJ, Sampath D, GuhaThakurta D, Savage H, Punnoose EA, et al. Predictive biomarkers of sensitivity to the phosphatidylinositol 3' kinase inhibitor GDC-0941 in breast cancer preclinical models. Clin Cancer Res 2010;16:3670–83. [PubMed: 20453058]

50. Juric D, Rodon J, Gonzalez-Angulo AM, Burris HA, Bendell JC, Berlin J, et al. BYL719,a next generation PI3K alpha specific inhibitor: Preliminary safety, PK, and efficacy results from the first-in-human study. Cancer Res 2012;72: CT–01.

51. Roper J, Richardson MP, Wang WV, Richard LG, Chen W, Coffee EM, et al. The dual PI3K/Mtor inhibitor NVP-BEZ235 induces tumor regression in a genetically engineered mouse model of PIK3CA wild-type colorectal cancer. PLoS One 2011;6:e25132. [PubMed: 21966435]

52. Mayer IA, Abramson VG, Formisano L, Balko JM, Estrada MV, Sanders ME, et al. A phase Ib study of alpelisib (BYL719), a PI3Kalpha-specific inhibitor, with letrozole in ER+/HER2− metastatic breast cancer. Clin Cancer Res 2017;23:26–34. [PubMed: 27126994]

53. Pollock N, Wang L, Wallweber G, Gooding WE, Huang W, Chenna A, et al. Increased expression of HER2, HER3, and HER2:HER3 heterodimers in HPV-positive HNSCC using a novel proximity-based assay: implications for targeted therapies. Clin Cancer Res 2015;21:4597–606. [PubMed: 26138066]

54. Abramson VG, Supko JG, Ballinger T, Cleary JM, Hilton JF, Tolaney S, et al. Phase Ib study of safety and pharmacokinetics of the PI3K inhibitor SAR245408 with the HER3 neutralizing human antibody SAR256212 in patients with solid tumors. Clin Cancer Res 2017;23:3520–8. [PubMed: 28031425]

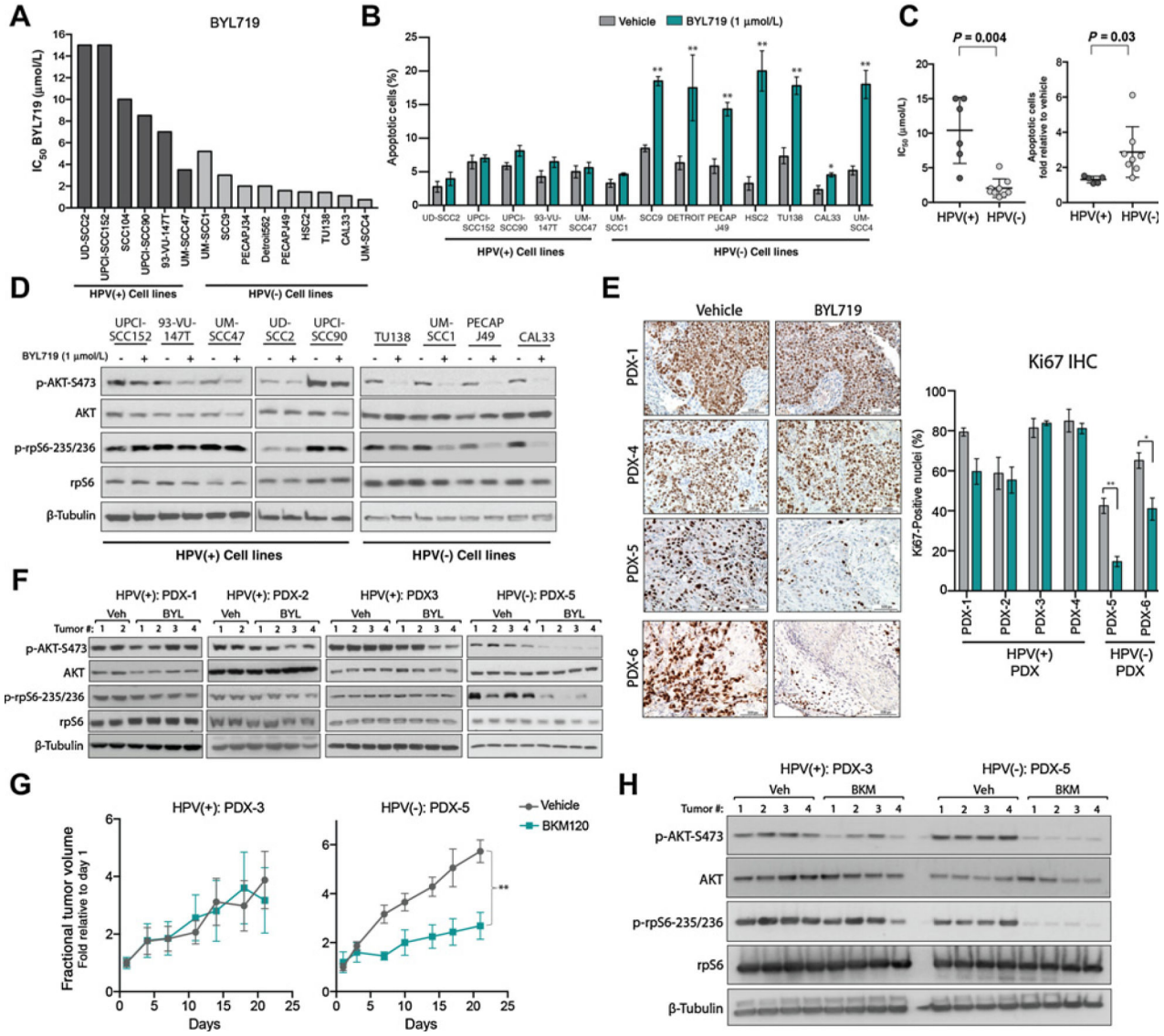

Figure 1.

HPV(+) preclinical models are less sensitive to PI3K inhibitors than HPV(−) models. **A,** IC_{50} for BYL719 effect on cellular proliferation of six HPV(+) and nine HPV(−) HNSCC cell lines after 72 hours of treatment. Data are representative of six replicates from three independent experiments. **B,** The percentage of Annexin V-positive/propidium iodide-negative cells was determined after 72 hours of vehicle or BYL719 (1.0 μmol/L) treatment of HPV(+) and HPV(−) cell lines. Data points represent the mean ± SEM of three independent experiments. *, $P < 0.05$; **, $P < 0.01$. **C,** Statistical comparisons of differences between IC_{50} values of BYL719 (left) and induction of apoptosis by BYL719 (right) on HPV(+) and HPV(−) cell lines. Each dot represents the mean of three independent experiments. **D,** Whole-cell lysates were harvested from five HPV(+) and four HPV(−) cell lines after 72 hours of vehicle or BYL719 (1.0 μmol/L) treatment, followed by immunoblotting for PI3K pathway proteins. **E,** Four HPV(+) PDXs (PDX-1, 2, 3, and 4) and two HPV(−) PDXs (PDX-5 and 6) were established in NSG mice and subsequently treated

daily with vehicle or BYL719 (20 mg/kg) for five days. Ki67 staining was evaluated by IHC and positive nuclei were quantified with Figi software (n = 4–6 tumors per treatment group were analyzed; representative sections from one of each group are shown). Tumors were stained with secondary antibody only as a control. Magnification, ×20. Scale bars, 500 px. Data are means ± SEM of three independent fields of view per tumor. *, $P < 0.05$; **, $P < 0.01$. **F,** Lysates from HPV(+) and HPV(−) PDXs treated for five days with vehicle or BYL719 (20 mg/kg) were subjected to immunoblotting for PI3K pathway proteins (representative tumors from each treatment group are shown). **G,** HPV(+) PDX-3 and HPV(−) PDX-4 were treated with vehicle or BKM120 (20 mg/kg) 5 days/week for 21 days. Tumor volumes were calculated as fractions of the average starting volume for each group, and the mean tumor volume ± SEM is shown (n = 6 tumors per treatment group). **, $P < 0.01$. **H,** Tumor lysates from **G** were immunoblotted for PI3K pathway proteins (4 tumors per treatment group are shown). (3-Tubulin was used as a loading control for all immunoblots. P values for all experiments were calculated using a two-tailed Student t test.

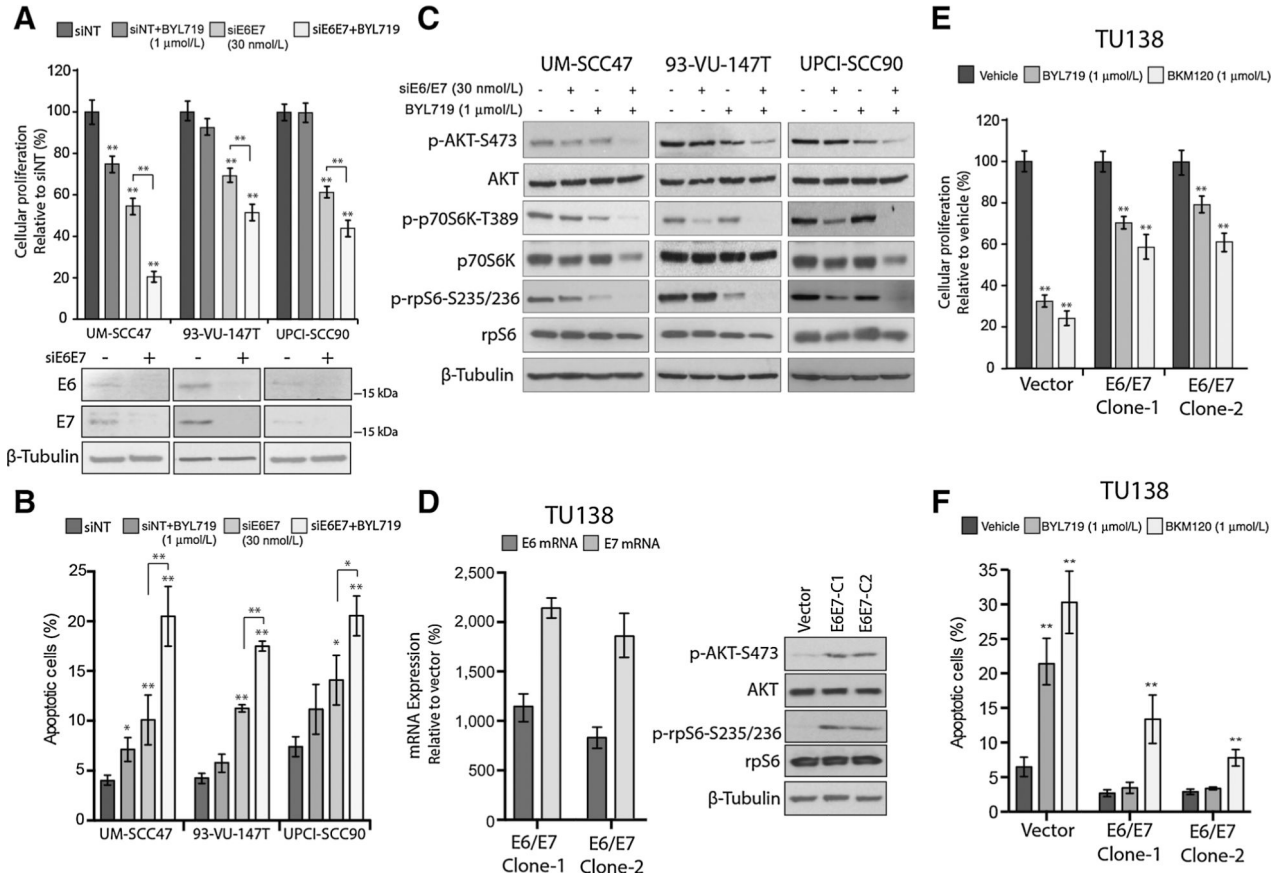

Figure 2.

HPV16 E6 and E7 oncoproteins mediate resistance to PI3K inhibitors. **A,** Three HPV(+) HNSCC cell lines were transfected with siE6E7 (30 nmol/L) or nontargeting siRNA (siNT) and treated with vehicle or BYL719 (1.0 μmol/L) for 72 hours before performing proliferation assays. Proliferation is plotted as a percentage of growth relative to siNT-transfected cells ($n = 6$ replicates in three independent experiments). Cell lysates were analyzed to confirm E6and E7 knockdown. **, $P < 0.01$. B, Three HPV(+) HNSCC cell lines were transfected with siE6E7 (30 nmol/L) or siNT and treated with vehicle or BYL719 (1.0 μmol/L) for 72 hours, followed by assessment of Annexin V/propidium iodide staining. Data points are represented as mean ± SEM of three independent experiments. *, $P < 0.05$; **, $P < 0.01$. C, Lysates from cells in **A** were immunoblotted for PI3K pathway proteins. **D,** The HPV(−) HNSCC cell line TU138 was transduced with virus expressing HPV16 E6 and E7 or a vector control, and expression of E6 and E7 mRNA transcripts was validated in two independent stable clones. Activation of the PI3K pathway in the clones was evaluated by immunoblot analysis. **E** and **F,** Two TU138 clones overexpressing E6 and E7 or vector control were treated with vehicle, BYL719 (1.0 μmol/L), or BKM120 (1.0 μmol/L) for 72 hours before assessing proliferation (**E**) or apoptosis (**F**). Data points are represented as mean ± SEM of three independent experiments. **, $P < 0.01$. β-Tubulin was used as a loading control for all immunoblots. *P* value for all experiments was calculated using two-tailed Student *t* test.

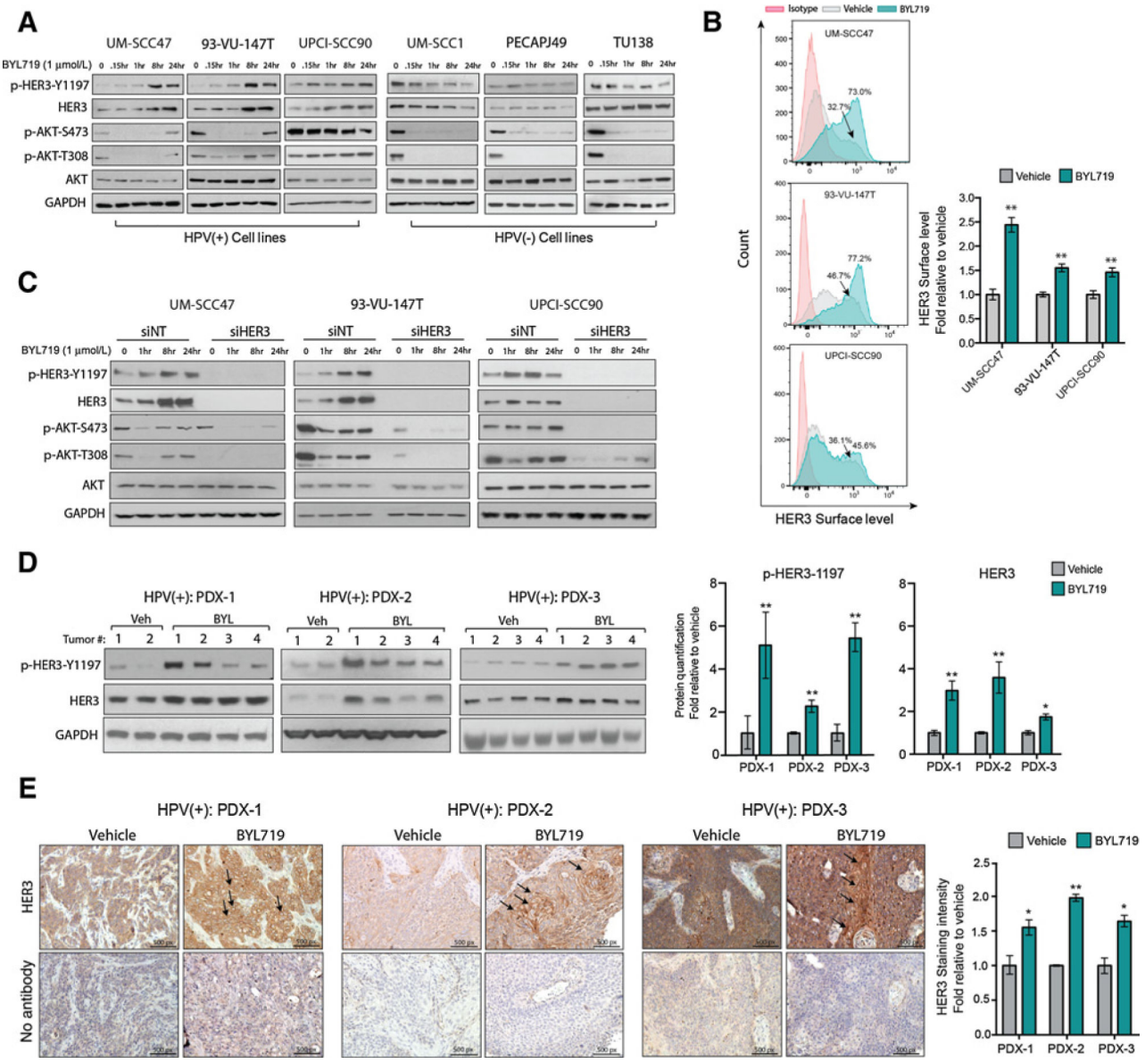

Figure 3.

PI3K inhibitors activate the HER3/AKT signaling pathway in HPV(+) HNSCC preclinical models. **A,** Three HPV(+) and HPV(−) cell lines were treated for the designated time points with vehicle or BYL719 (1.0 μmol/L), followed by immunoblotting for the indicated proteins. **B,** HER3 surface level expression was examined by flow cytometry after 24 hours of vehicle or BYL719 (1.0 μmol/L) treatment in HPV(+) cell lines. Representative histograms with percent increases in HER3 surface expression are shown. Cells were stained with a matched isotype antibody as a control. The bar graph depicts the average HER3 membrane levels from three independent experiments, **, $P < 0.01$. **C,** HPV(+) cell lines were transfected with siNT or siHER3 (30 nmol/L) for 48 hours, then treated with vehicle or BYL719 (1.0 μmol/L) for the indicated time points, followed by immunoblot analysis. **D,** Lysates from HPV(+) PDXs (PDX-1, 2, and 3) treated for 5 days with vehicle or BYL719 (20 mg/kg) were subjected to immunoblotting for indicated proteins (representative tumors

from each treatment group are shown). Blots were quantified with Figi software and normalized to GAPDH. *, $P < 0.05$; **, $P < 0.01$. **E,** HER3 staining was evaluated by IHC in tumors from **D**. Black arrows, strong HER3 membrane staining. Tumors were stained with secondary antibody only as a control and quantified with Figi software ($n = 4$–6 tumors per treatment group were analyzed; representative sections from one of each group are shown). Magnification, ×20. Scale bars, 500 px. Data are means ± SEM of three independent fields of view per tumor. *, $P < 0.05$ or **, $P < 0.01$. All cell line experiments were run in triplicate, and GAPDH was used as a loading control. *P* value was calculated using two-tailed Student *t* test.

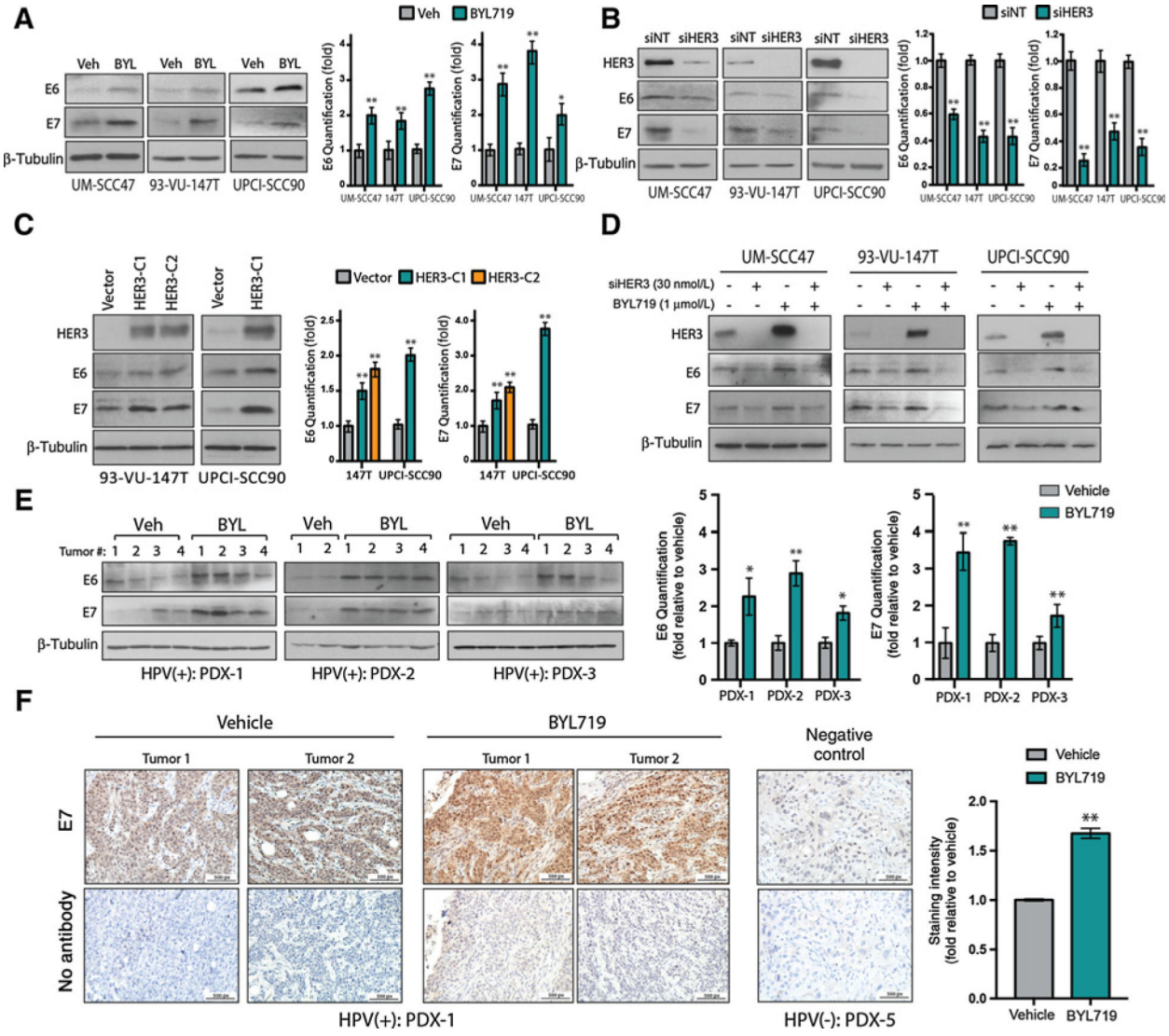

Figure 4.

HER3 regulates the abundance of E6 and E7 in HPV(+) preclinical models. **A,** Three HPV(+) cell lines were treated with vehicle or BYL719 (1.0 μmol/L) for 24 hours, followed by immunoblotting for E6 and E7. **B,** HPV(+) cell lines were transfected with siNT or siHER3 (30 nmol/L) for 72 hours, followed by immunoblotting for the indicated proteins. **C,** pLX302-HER3 or a vector control were stably overexpressed in the HPV(+) cell lines 93-VU-147T and UPCI-SCC90. Lysates were harvested from vector and two HER3 stable clones (HER3-C1 and HER3-C2) for 93-VU-147T and one HER3 stable clone for UPCI-SCC90 and immunoblotted for the indicated proteins. **D,** Three HPV(+) cell lines were transfected with siNT or siHER3 for 48 hours, followed by treatment with BYL719 (1.0 μmol/L) for 24 hours. Lysates were harvested and immunoblotted for the indicated proteins. **E,** Lysates from HPV(+) PDXs (PDX-1, 2, and 3) treated for five days with vehicle or BYL719 (20 mg/kg) were subjected to immunoblotting for E6 and E7 (representative tumors from each treatment group are shown). **F,** E7 staining was evaluated by IHC in tumors from **E**. HPV(−) PDX-5 was used as a negative control and all tumors were stained with

secondary antibody only. Staining intensity was quantified with Figi software (n = 4–6 tumors per treatment group were analyzed; representative sections from one of each group are shown). Magnification, ×20. Scale bars, 500 px. Data are means ± SEM of three independent fields of view per tumor. *, $P < 0.05$; **, $P < 0.01$. Figi software was used to quantify E6 and E7 protein abundance in all immunoblots; bar graphs represent the mean ± SEM of three independent cell line experiments and of each treatment group for PDX experiments. *, $P < 0.05$; **, $P < 0.01$ by two-tailed Student t test. β-Tubulin was used as a loading control for immunoblots.

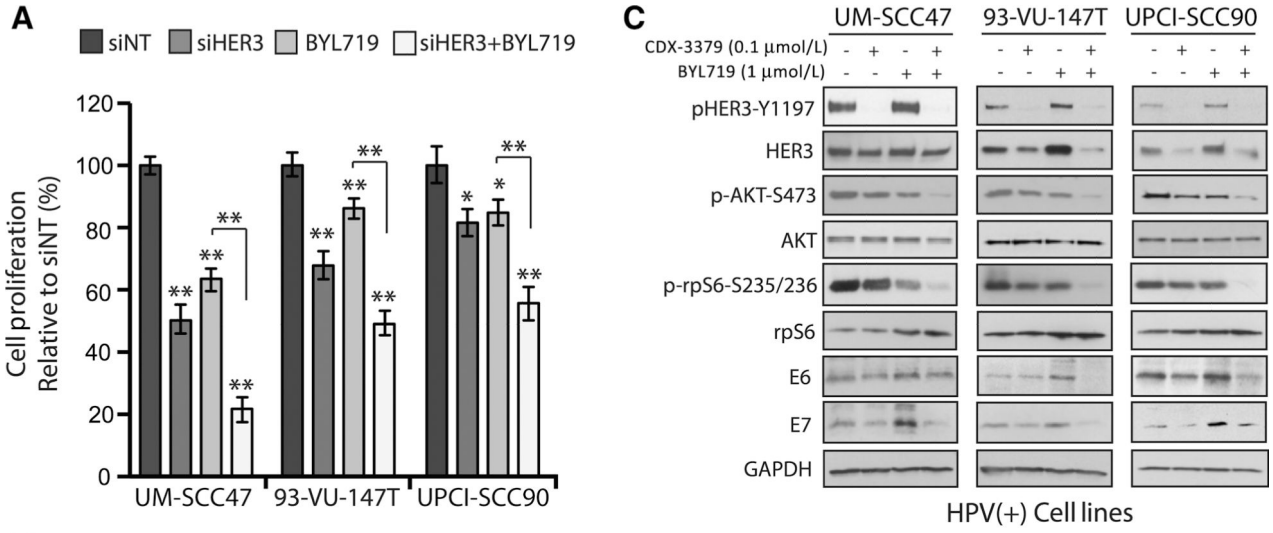

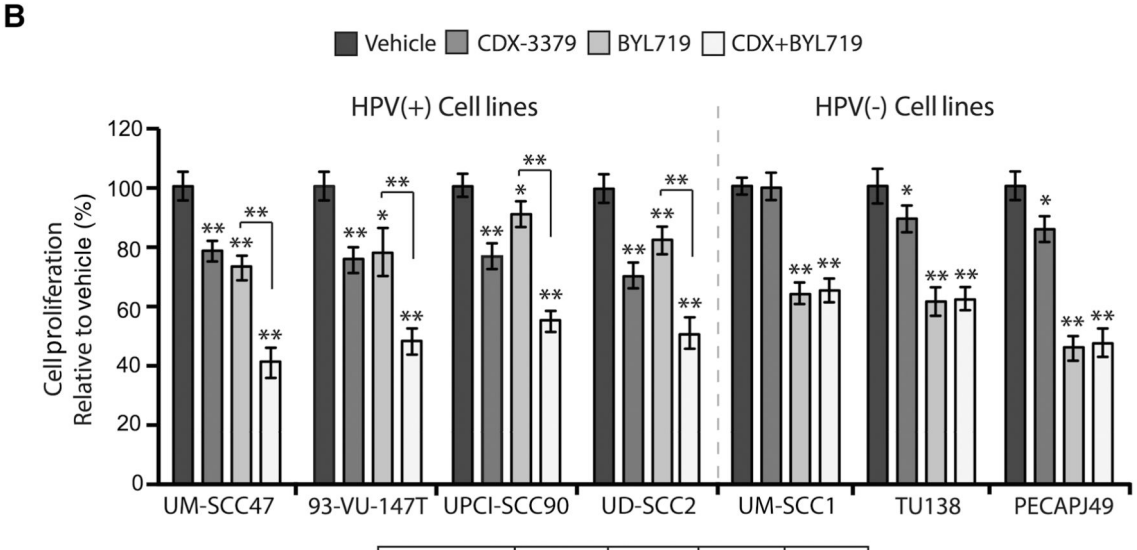

Cell line	Expected	Observed	Ratio	Synergy
UM-SCC47	0.59	0.41	0.69	YES
93-VU-147T	0.60	0.48	0.80	YES
UPCI-SCC90	0.70	0.58	0.82	YES
UD-SCC2	0.57	0.51	0.89	YES

Figure 5.

Targeting HER3 enhances the efficacy of PI3K inhibitors and sustains knockdown of the PI3K pathway. **A,** Three HPV(+) HNSCC cell lines were transfected with siNT or siHER3 (30 nmol/L) and treated with vehicle or BYL719 (1.0 µmol/L) for 72 hours before performing proliferation assays. Proliferation is plotted as a percentage of growth relative to siNT-transfected cells ($n = 3$ replicates in three independent experiments). **B,** Four HPV(+) and three HPV(−) cell lines were treated with vehicle, CDX-3379 (0.1 µmol/L), BYL719 (1.0 µmol/L), or the combination for 72 hours before assessing proliferation ($n = 6$ replicates in three independent experiments). Synergy of the combination was determined using the fractional product method. A ratio of observed to expected values less than 1 indicates

synergism. **C,** HPV(+) cell lines were treated with vehicle, CDX-3379 (0.1 μmol/L), BYL719 (1.0 μmol/L), or the combination for 24 hours before immunoblotting for the indicated proteins. All data points are represented as mean ± SEM. *, $P < 0.05$; **, $P < 0.01$, by two-tailed Student t test. GAPDH was used as the loading control for all immunoblots.

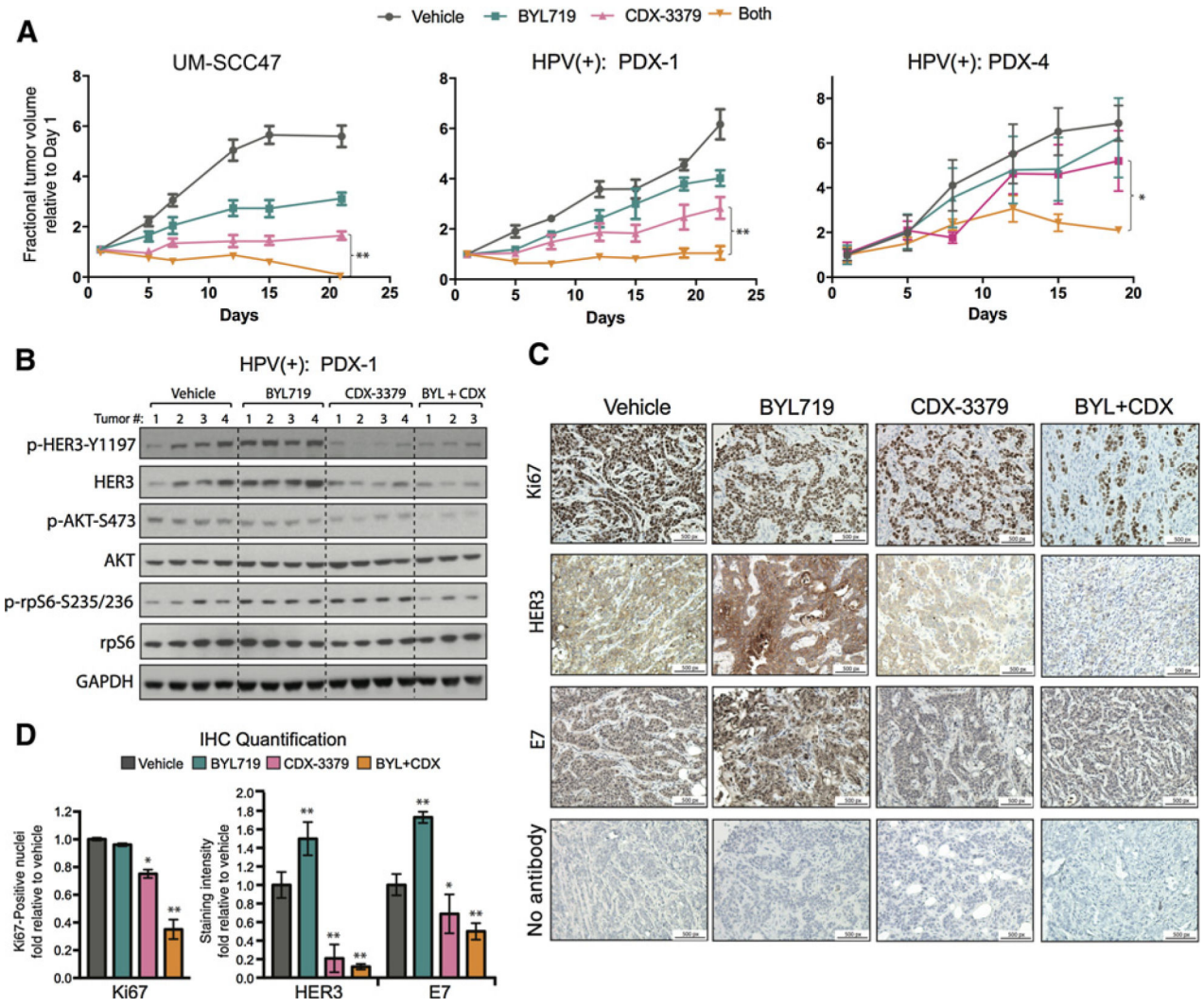

Figure 6.

Targeting HER3 overcomes PI3K-inhibitor resistance in HPV(+) HNSCC *in vivo* models. **A,** The HPV(+) cell line, UM-SCC47, and HPV(+) PDXs (PDX-1 and 4) were established in either athymic nude mice or NSG mice and subsequently treated with vehicle, BYL719 (20 mg/kg), CDX-3379 (10 mg/kg), or the combination for the indicated time periods. Tumor volumes were calculated as fractions of the average starting volume for each group, and the mean tumor volume ± SEM is shown ($n = 5–8$ tumors per treatment group). *, $P < 0.05$; **, $P < 0.01$, by two-tailed Student t test. **B,** HPV(+) PDX-1 tumors were harvested three hours after the last treatment, followed by immunoblotting for the indicated proteins (representative tumors from each treatment group are shown). **C,** Ki67, HER3, and E7 were evaluated by IHC in HPV(+) PDX-1 tumors. Tumor sections were stained with secondary antibody only as a control. Magnification, ×20. Scale bars, 500 px. Representative sections from one of each group are shown. **D,** Quantification of IHC in **C** was performed using Figi software ($n = 4–6$ tumors per treatment group were analyzed). Data are means ± SEM of three independent fields of view per tumor.